



Non-steroidal dissociated glucocorticoid agonists: indoles as A-ring mimetics and function-regulating pharmacophores

Raj Betageri^{a,*}, Thomas Gilmore^a, Daniel Kuzmich^a, Thomas M. Kirrane^a, Jörg Bentzien^a, Dieter Wiedenmayer^a, Younes Bekkali^a, John Regan^a, Angela Berry^a, Bachir Latli^a, Alison J. Kukulka^a, Tazmeen N. Fadra^a, Richard M. Nelson^a, Susan Goldrick^b, Ljiljana Zuvela-Jelaska^b, Don Souza^b, Josephine Pelletier^b, Roger Dinallo^c, Mark Panzenbeck^c, Carol Torcellini^c, Heewon Lee^a, Edward Pack^a, Christian Harcken^a, Gerald Nabozny^b, David S. Thomson^a

^a Department of Medicinal Chemistry, Boehringer Ingelheim Pharmaceuticals, Inc., 900 Ridgebury Road, Ridgefield, CT 06877, USA

^b Department of Immunology and Inflammation, Boehringer Ingelheim Pharmaceuticals, Inc., 900 Ridgebury Road, Ridgefield, CT 06877, USA

^c Drug Discovery Support, Boehringer Ingelheim Pharmaceuticals, Inc., 900 Ridgebury Road, Ridgefield, CT 06877, USA

ARTICLE INFO

Article history:

Received 7 August 2011

Revised 1 September 2011

Accepted 6 September 2011

Available online 10 September 2011

Keywords:

Non-steroidal glucocorticoid agonist

Dissociated activity

Function-regulating pharmacophore

ABSTRACT

We report a SAR of non-steroidal glucocorticoid mimetics that utilize indoles as A-ring mimetics. Detailed SAR is discussed with a focus on improving PR and MR selectivity, GR agonism, and in vitro dissociation profile. SAR analysis led to compound (*R*)-**33** which showed high PR and MR selectivity, potent agonist activity, and reduced transactivation activity in the MMTV and aromatase assays. The compound is equipotent to prednisolone in the LPS-TNF model of inflammation. In mouse CIA, at 30 mg/kg compound (*R*)-**33** inhibited disease progression with an efficacy similar to the 3 mg/kg dose of prednisolone.

© 2011 Elsevier Ltd. All rights reserved.

The glucocorticoid receptor (GR), a member of the nuclear receptor family, is an attractive drug discovery target, and chemical entities that function as GR agonists and antagonists have therapeutic potential. Research in the last decade has led to a better understanding of molecular mechanisms that mediate functions of the GR.^{1–7} Transrepression (TR) promotes downregulation of target genes that encode cytokines, cell adhesion molecules and enzymes, and TR is thought to be predominantly involved in mediating the anti-inflammatory effects of the GR.^{8–10} Overactivation of certain transcriptional genes, known as transactivation (TA), has been implicated in the deleterious side effects of glucocorticoids (GCs).^{11,12} The concept, 'dissociated GR ligand' has evolved out of a suggestion that it is feasible to design GR ligands that display differential effects on TR and TA pathways. A therapy based on such dissociated GR agonists is anticipated to give the desired outcome of anti-inflammatory effect similar to prednisolone but with decreased side effects. At a molecular level, designing a dissociated GR ligand entails optimized positioning of function-regulating pharmacophores (FRPs) in addition to achieving a suitable size and shape of the ligand.

As a result, identifying non-steroidal dissociated GR agonists has been a goal sought by drug discovery efforts for some time. Several reports disclosing novel non-steroidal GR ligands from different structural classes have appeared in the literature.^{13–24} Recent review articles^{25–27} summarize different chemotypes that function as GR agonists with a dissociated profile.

Identification of trifluoromethylcarbinol group as a pharmacophore essential for the agonist activity of GR ligands can be characterized as one of the significant discoveries in the development of GR modulators. Disclosure of ZK216438 (+ enantiomer) as a dissociated GR ligand spurred extensive research activity that has led to the discovery of multiple classes of GR agonists containing trifluoromethylcarbinol group. Summarized accounts of the activity profiles of these compounds can be found in the GR literature.^{26–29} Selected examples of trifluoromethylcarbinol containing GR agonists are shown in Figure 1. In addition to identifying several A- and D-ring mimics, these studies have provided insight into the binding modes of various non-steroidal GR agonists. X-ray structures of GR ligand binding domain (GR-LBD) co-crystals with **GSK1**³⁰ and **GSK2**³¹ have been solved which have helped in establishing the role of trifluoromethylcarbinol in these ligands. Hydroxyl group of trifluoromethylcarbinol moiety corresponds to the steroidal 11-β-OH and the previously hypothesized hydrogen bonding interaction with Asn564 is now confirmed by these

* Corresponding author. Tel.: +1 203 798 5428.

E-mail address: raj.betageri@boehringer-ingenheim.com (R. Betageri).

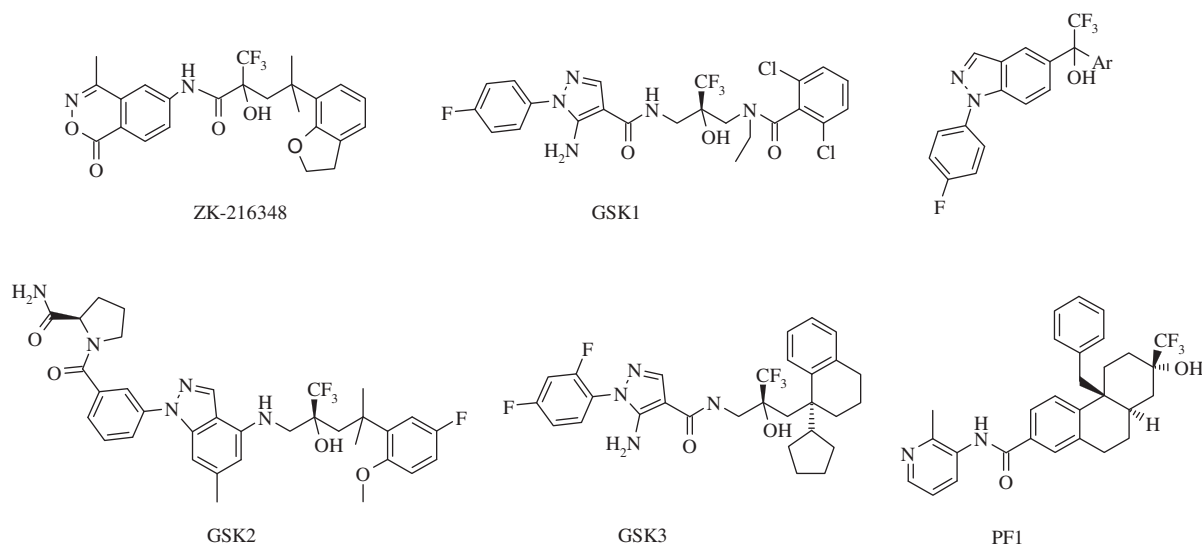


Figure 1. Known non-steroidal GR agonists containing trifluoromethylcarbinol pharmacophore.

X-ray crystal studies. Our previous report showed that replacing the trifluoromethyl group with a benzyl or cyclohexyl moiety in a GR ligand related to ZK216348 alters the functional profile from agonist to an antagonist.³² Some of the dissociated GR ligands currently in the clinical trials are likely to be trifluoromethylcarbinol derivatives which highlight their prominent role in the discovery of non-steroidal glucocorticoid mimetics.

Our quest for receptor selective, dissociated GR ligands utilized ZK216348 as the starting point and the SAR studies led to the discovery of compound **1** (Fig. 2).^{33,34} Compound **1** was reported as a potent GR ligand but one that displayed poor selectivity over PR and MR. In the *in vitro* assays **1** is a partial agonist and shows a dissociated profile. The docking pose of a closely related analogue of **1**, generated by docking that compound into the GR–LBD derived from the GR–LBD dexamethasone co-crystal X-ray structure, suggests that the left-hand side (LHS) phenyl ring of **1** and the A-ring of dexamethasone overlay. In addition, SAR studies of **1** revealed that subtle changes in the substitution patterns on the LHS phenyl ring have a dramatic effect on the agonist activity, consistent with literature data where steroid A-ring mimics are reported to play a crucial role in influencing the agonist activity. We set out to explore different A-ring replacements in compound **1** as an initial step towards identifying novel dissociated GR ligands. A quick survey of aromatic heterocyclic rings such as 2-benzofuran, 2-benzothiophene, 2-benzimidazole and 2-indole identified compound **2** as a potent GR agonist.³⁵ Compound **2** showed no detectable binding to AR at 1.1 μM but it lacks the desired nuclear receptor selectivity over PR and MR (Table 1). In the *in vitro* transactivation assay compound **2** is not dissociated. However, full agonist properties of this ligand, as reflected by both the IC_{50} and % maximal efficacy in the TR assays, make this an attractive candidate for further optimization.³⁶ Accordingly, SAR studies were initiated aimed at improving the PR and MR selectivity and *in vitro* dissociation profile of the GR agonist **2**.

To gain insight into binding interactions of **2** with the GR–LBD, (R)-**2** was docked^{37–39} into the GR–LBD using the dexamethasone GR–LBD co-crystal X-ray structure.⁴⁰ The indole and 2-methoxy-5-fluoro groups of (R)-**2** and the A- and D-rings, respectively, of dexamethasone overlay (Fig. 3a and b). A common interaction for the two ligands involves the Asn564 side chain, where the central hydroxyl of (R)-**2** and the 11- β -OH of dexamethasone overlay and are suggested to hydrogen bond the Asn564 side chain. Key interactions that engage the network of the Gln570/Arg611

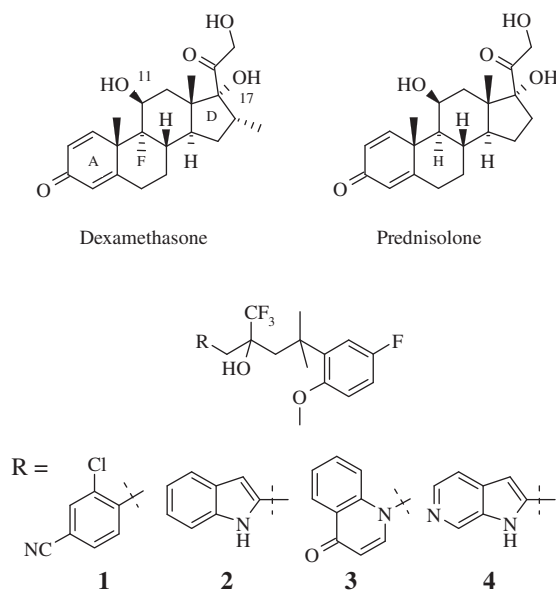
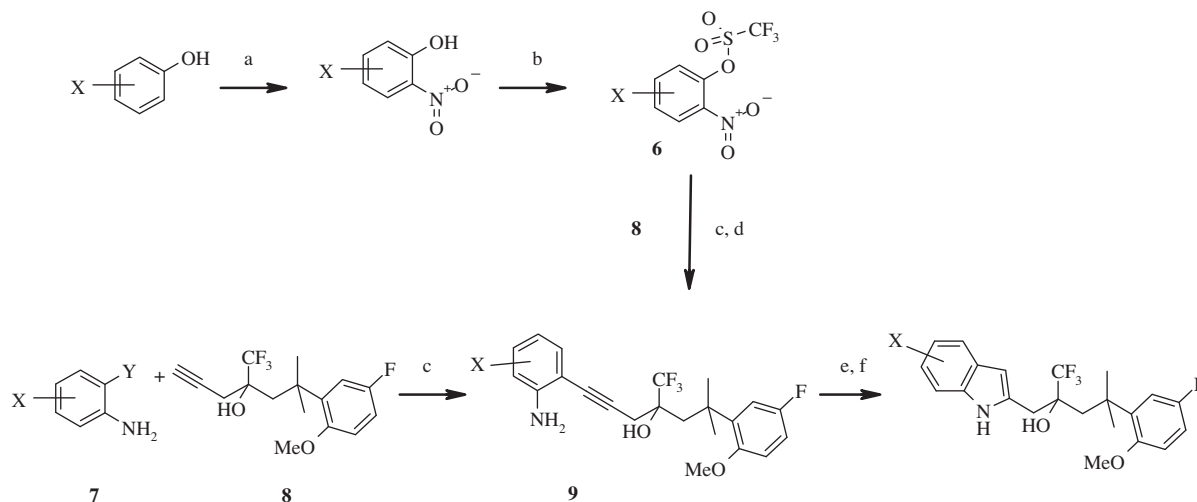


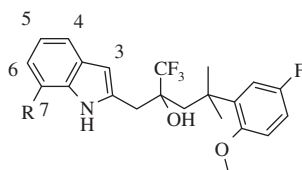
Figure 2. Steroidal and non-steroidal glucocorticoid agonists.

residues and the A-ring carbonyl are observed for dexamethasone. The C-5 and C-6 carbon atoms of the indole ring are in proximity to the Gln570/Arg611 residues but lacking a hydrogen bond acceptor at either of these positions (R)-**2** cannot participate in an interaction similar to the A-ring carbonyl of dexamethasone. Instead, a potential hydrogen bond between the indole NH and the Leu563 backbone carbonyl is implicated by the model (Fig. 3a). Adjacent to the indole NH is the C-7 carbon and the presence of the *iso*-butyl side chain of Leu566 is suggested in the surrounding binding region. The binding region at the C-4 position of the indole ring is hydrophobic with the presence of the Ile608 and Phe623 side chains. At the D-ring region, no key interactions between the 2-methoxy-5-fluoro ring and the GR–LBD (Fig. 3b) are identified. A design approach was formulated that utilizes our binding hypothesis and exploits the scope of literature reports that describe small structural changes to ligands can have significant effects on the functional profile.^{41–44} We set out to examine the effect of substitution by small groups such as F, CH_3 , CF_3 and cyano on the indole



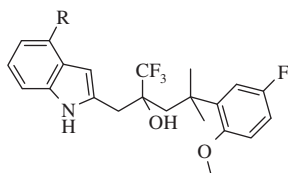
Scheme 1. Reagents and conditions: (a) $\text{NO}_2^+ \text{BF}_4^-$, MeCN, 0 °C, 1 h; (b) $(\text{CF}_3\text{SO}_2)_2\text{O}$, NEt_3 , CH_2Cl_2 , 0 °C, 2 h; (c) $\text{Pd}(\text{PPh}_3)_2\text{Cl}_2$ (0.05 equiv), CuI (0.1 equiv), NEt_3 , MeCN, rt, 1–15 h; (d) Fe , $\text{CH}_3\text{CO}_2\text{H}$, 60 °C, 30 min; (e) $(\text{CF}_3\text{CO}_2)_2\text{O}$, CH_2Cl_2 , 0 °C; (f) anhydrous K_2CO_3 , DMSO, 140 °C, microwave, 15 min.

Table 2
7-Substituted indoles



Compd	R	IC ₅₀ (nM)			IC ₅₀ (nM), (% efficacy) IL-6 inhibition	EC ₅₀ (nM), (% efficacy) Aromatase induction
		GR	PR	MR		
2	H	22	290	383	7 (87)	23 (93)
10	F	15	930	435	36 (75)	473 (89)
11	CH ₃	56	1450	1035	>2000 (26)	>2000 (26)
12	CF ₃	120	1750	1650	>2000	>2000
13	CN	27	>2000	1420	>2000 (30)	>2000

Table 3
4-Substituted indoles

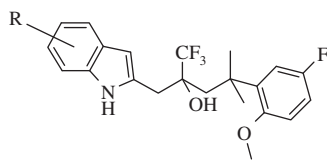


Compd	R	IC ₅₀ (nM)			IC ₅₀ (nM), (% efficacy) IL-6 inhibition	EC ₅₀ (nM), (% efficacy) Aromatase induction
		GR	PR	MR		
2	H	22	290	383	7 (87)	23 (93)
14	CH ₃	30	350	415	6 (91)	9 (110)
15	CF ₃	160	>2000	>2000	290 (70)	IP* (30)
16	CN	5	440	225	8 (91)	21 (91)
17	Et	28	1000	790	88 (90)	IP (49)

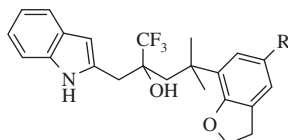
* Indeterminate potency as a result of no defined inflexion point in the dose response curve.

The dihydrobenzofuran (DBF) analogues **26–30** (Table 5) were prepared following previously described procedures.³³ The synthesis of DBF analogue **33** was carried out according to Scheme 2. Compounds **31** and **32** were prepared following a similar procedure. Thus, the intermediate diol **34a** prepared by following the

previously described procedures^{35,45} was converted to the corresponding acetone. Halogen-metal exchange using *n*-BuLi followed by treatment with dimethyldisulfide and deprotection of the acetone gave the sulfide **34b**. Cleavage of the vicinal diol and concomitant oxidation of the sulfide to give the

Table 4
5- and 6-Substituted indoles

Compd	R	IC ₅₀ (nM)			IC ₅₀ (nM), (% efficacy)	EC ₅₀ (nM), (% efficacy)	EC ₅₀ (nM), (% efficacy)
		GR	PR	MR	IL-6 inhibition	Aromatase induction	MMTV induction
Dexamethasone	—	3	>2000	33	0.51 (100)	1.8 (100)	17 (100)
Prednisolone	—	15	>2000	44	7 (96)	19 (92)	16 (91)
2	H	22	290	383	7 (87)	23 (93)	—
18	5-F	24	405	405	78 (84)	94 (98)	—
19	5-CH ₃	66	1800	1250	113 (86)	230 (104)	—
20	5-CF ₃	290	>2000	>2000	191 (77)	640 (65)	—
21	5-CN	8	815	415	11 (89)	28 (81)	—
(<i>R</i>)- 21	5-CN	1	155	45	3 (90)	6 (71)	36 (10)
22	6-F	30	265	350	29 (94)	33 (84)	—
23	6-CH ₃	38	1250	720	334 (60)	976 (70)	—
24	6-CF ₃	77	1600	910	>2000	>2000	—
25	6-CN	14	395	435	14 (91)	113 (98)	—

Table 5
Substituted Dihydrobenzofuran Analogues

Compd	R	IC ₅₀ (nM)			IC ₅₀ (nM), (% efficacy)	EC ₅₀ (nM), (% efficacy)
		GR	PR	MR	IL-6 inhibition	Aromatase induction
26	H	19	225	400	10 (83)	311 (103)
27	F	8	255	265	21 (90)	125 (98)
28	CH ₃	10	145	240	7 (95)	16 (105)
29	Br	32	415	585	16 (88)	45 (99)
30	CN	15	710	405	104 (65)	356 (55)
31	SO ₂ CH ₃	6	>2000	610	100 (84)	>2000* (20)

* Data reflects MMTV Induction in HeLa, EC₅₀ (nM), efficacy % versus dex.

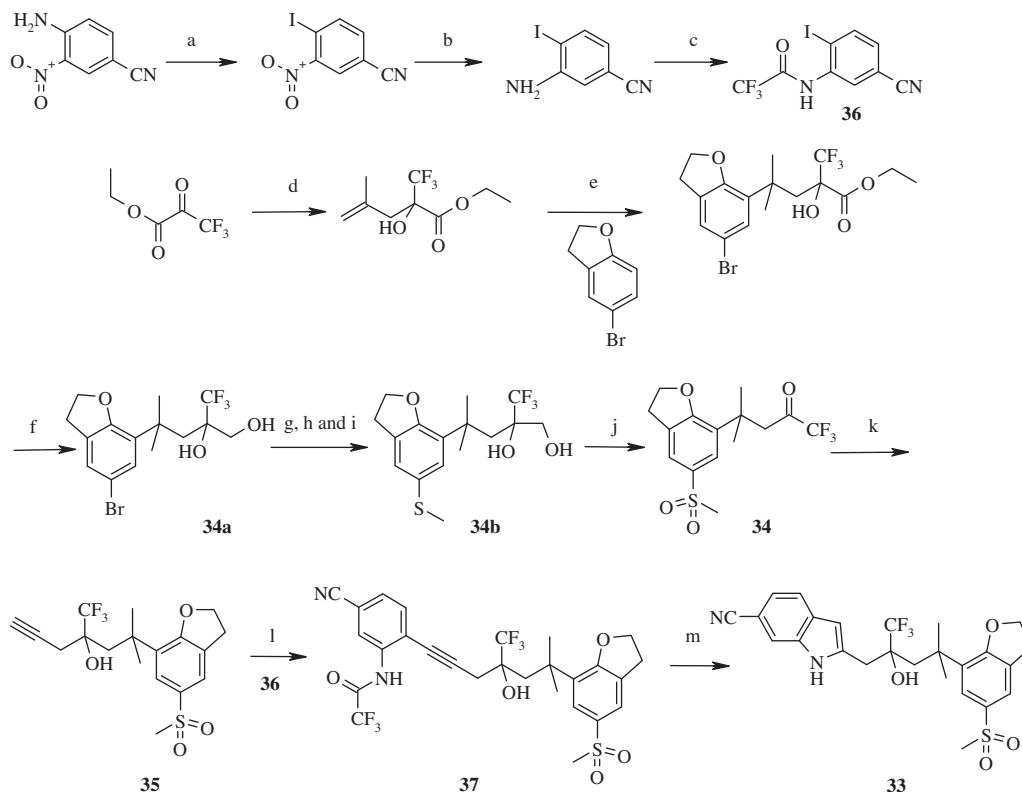
methylsulfone-DBF-trifluoromethyl ketone **34** was carried out by a two stage oxidation employing NaO₄ and RuCl₃. Subsequent elaboration of **34** gave the alkyne **35**, which was subjected to Sonogashira coupling with the iodo derivative **36**, synthesized according to literature protocols (Scheme 2). Cs₂CO₃ mediated cyclization of the resulting intermediate **37** led to the racemic 6-cyano indole analogue **33**. The chiral separation on a Chiralpak AD-H preparative column using 20% isopropanol in hexanes provided the eutomer (*R*)-**33** as the second eluting peak.

Nuclear receptor binding affinity of the target compounds was determined by their ability to compete for receptor binding with tetramethylrhodamine labeled dexamethasone (GR, MR) or mifepristone (PR) or ³H-testosterone (AR).⁴⁸ The transrepression potential was measured in human foreskin fibroblast (HFF) cells. Inhibition of IL-1 stimulated IL-6 production and percent efficacy was measured relative to dexamethasone, where inhibition by dexamethasone was set to 100%.^{49,50}

Achieving full therapeutic potential of synthetic GC mimetics is only accomplished by reducing TA activity in addition to enhancing nuclear receptor selectivity and agonist activity. A successful clinical outcome would then depend upon establishing an in vitro/in vivo (clinical) correlation to determine what level of in vitro dissociation is necessary to achieve the desired dissociation in vivo (in

the clinic). Two factors could be important in this regard. The first factor relies on identifying appropriate markers for evaluating in vitro transactivation. Our transactivation assays employ the MMTV promoter and aromatase⁵¹ as markers of gene activation. The compounds were counter screened for the induction of aromatase in HFF cells⁵² and the ability to activate the MMTV promoter in HeLa cells transfected with a MMTV luciferase construct.^{25,53–57} Comparisons with dexamethasone establish a basis for identifying compounds with a dissociated profile. The second factor relates to the required level of separation between the transrepression and transactivation activities that could qualify as in vitro dissociation. Broadly, dissociation can be defined as weak potency or low % maximal efficacy or both in transactivation assays compared to transrepression assays.

Since the racemic compound **2** and eutomer (*R*)-**2** displayed similar activity, SAR studies were performed using racemic compounds. Initially, we prepared N-methyl and C-3 linked indole analogues (data not shown) which showed no agonist activity in the cellular assay while displaying good GR affinity. Introducing CH₃, CF₃ and cyano groups at C-7 (Table 2, compounds **11**, **12** and **13**), which is proximal to the indole NH, has a similar effect as good binding affinity did not translate into agonist activity. Thus, blocking the indole NH (N-Me analogue) or introducing steric



Scheme 2. Reagents and conditions: (a) NaNO_2 , NaI , 30% H_2SO_4 , DMSO , 0°C ; (b) SnCl_2 , EtOH , 90°C , 3 h; (c) $(\text{CF}_3\text{CO}_2)_2\text{O}$, CH_2Cl_2 , 0°C ; (d) THF , -65°C , then methylallylmagnesium chloride (1.3 equiv), 4 h, rt, 12 h, 61%; (e) $\text{ClCH}_2\text{CH}_2\text{Cl}$, AlCl_3 at 0°C , then rt, 12 h, 30%; (f) LiAlH_4 , THF , 48 h; (g) 2,2-dimethoxypropane, *p*-toluenesulfonic acid; (h) *n*- BuLi , -78°C , $(\text{MeS})_2$, 2 h; (i) methanolic HCl , CF_3 ; (j) NaIO_4 , RuCl_3 , MeCN , rt, 5 h; (k) Al , HgCl_2 , THF , propargyl bromide, 40°C , 1 h, 3 h, rt; (l) **36** (1 equiv), $\text{Pd}(\text{PPh}_3)_2\text{Cl}_2$ (0.05 equiv), CuI (0.1 equiv), NEt_3 , THF , 0°C to rt, 2 h; (m) Cs_2CO_3 , DMSO , 100°C , 3 h.

demand at the indole NH (7-substituted analogues) is detrimental for the agonist activity. These results confirm the importance of the indole NH–Leu563 interaction for the agonist activity, which is suggested by the docking studies (Fig. 3a). A fluorine atom, a hydrogen atom isostere, does not have the same effect at C-7 and compound **10** displays good GR binding and agonist activity. These results reinforce the often observed lack of correlation between GR binding affinity and agonist activity.^{58–60} 7-substituted indoles (**10–13**) are more selective over PR than **2**. In the aromatase assay, 7-F compound **10**, the lone C-7 substituted agonist, is deemed dissociated with a 10-fold separation of $\text{EC}_{50}/\text{IC}_{50}$. Although the in vitro profile reflects receptor selectivity and dissociation, compound **10** was not advanced to in vivo studies because of poor PK properties (data not shown).

Substitutions at carbon C-4 of the indole ring, which is on the opposite side of the indole NH, are not detrimental for agonist activity and the compounds display IC_{50} in the range 6–290 nM (**14–17**, Table 3) and maximal efficacies greater than 70%. Increasing the size of the substitution from methyl, ethyl and CF_3 results in incremental reductions of the agonist potency (compare **14**, **17** and **15**) suggesting a limitation in the size of the binding pocket near the C-4 position of the indole. The cyano analogue **16** displays 90-fold PR selectivity, and potent agonist activity unlike the C-7 cyano analogue **13**. The cyano analogue **16** is not dissociated in the aromatase assay. The 4- CF_3 and 4-ethyl analogues (**15** and **17**) show maximal efficacies of 30% and 49%, respectively, and are classified as dissociated in the aromatase assay. But the 30-fold GR/PR selectivity for the ethyl analogue **17** was considered less than optimal.

As discussed earlier, our model suggests that the A-ring of dexamethasone and the indole ring of (*R*)-**2** overlay with the A-ring

carbonyl of the former residing in a space closer to the C-5 and C-6 carbon atoms of the latter. Compound (*R*)-**2** cannot interact with the Arg611/Gln570 pair in a manner similar to dexamethasone as indole ring of the former lacks hydrogen bond acceptor at either C-5 or C-6 position. Presence of hydrogen bond network between the A-ring mimics of non-steroidal GR agonists and the Arg611/Gln570 pair is established by the X-ray structures of GR–LBD co-crystals with **GSK1**³⁰ and **GSK2**³¹ (Fig. 1). Because of the suggested proximity of the Arg611/Gln570 pair to the C-5 or C-6 positions of the indole ring in **2**, it is expected that substitutions at C-5 or C-6 positions to affect the activity profile of **2**. While a fluorine atom at C-5 or C-6 has little effect on the GR binding affinity and agonist activity (Table 4), (**18** and **22**), introducing lipophilic groups such as CH_3 and CF_3 in the vicinity of Arg611/Gln570 pair is detrimental for the activity. The effect is more pronounced at C-6. While the 6- CH_3 and 6- CF_3 analogues (**23**, **24**) have GR binding affinity similar to **2**, 6- CH_3 compound **23** is a partial agonist (IC_{50} 334 nM, 60%) and 6- CF_3 compound **24** is devoid of agonist activity. These results perhaps suggest a disruption of the agonist conformation of GR–LBD complex with **23** and **24**. In contrast, both 5- CH_3 and 5- CF_3 analogues (**19**, **20**, Table 4) display agonist activity, but incremental loss in both the binding affinity and agonist activity is observed on increasing the size of the substitution from CH_3 to CF_3 . Introducing a hydrogen bond acceptor, cyano group, at C-5 or C-6 is not detrimental and both 5-CN and 6-CN analogues **21** and **25** display potent GR binding affinity and agonist activity (Table 4). While the agonist activity of **21** and **25** is comparable to that of the unsubstituted indole analogue **2**, improvement in selectivity over PR, MR is observed for both the compounds **21** and **25**. 100-fold PR selectivity and 50-fold MR selectivity is seen for 5-CN compound **21**, which reflects a pronounced effect

for 5-CN compared to 6-CN analogue **25** (~30-fold for PR and MR). A hypothesis based on the amino acid residue differences in the ligand binding domains of GR, PR and MR could explain the observed receptor selectivity data. The residue corresponding to Cys622 (binding pose in Fig. 3a) in GR–LBD is Tyr777 in PR–LBD and Tyr828 in MR–LBD. Interaction of the 5-CN with the Arg611/Gln570 pair in PR and MR could lead to movement of the Tyr side chain resulting in unfavorable interactions and loss in the binding affinity for PR and MR. In the aromatase assay, the 5-CN compound **21** is not dissociated (28 nM, 81%) but the 6-CN indole **25** displays an 8-fold higher EC₅₀ (113 nM, 98%) than the IL-6 IC₅₀ (14 nM, 91%). But the eutomer (*R*)-**21** of the 5-CN compound exhibits a maximal efficacy of 10% in the MMTV assay indicating a dissociated profile based on the % maximal efficacy.

Having identified the 5-CN analogue (*R*)-**21** as a PR, MR selective GR agonist with a dissociated profile in the MMTV assay, SAR was shifted to the RHS of the molecule **2** to assess the effect of RHS modifications and identify a broader panel of dissociated analogues of **2**. For this purpose we initially decided to use the unsubstituted indole ring at the LHS for the SAR studies. Docking shows that (Fig. 3b), the phenyl ring of (*R*)-**2** lies proximal to the steroid D-ring domain suggesting opportunities for potential interactions with Thr739. Our attention was drawn to the DBF ring, since a dissociated GR agonist ZK216348 with a DBF moiety has been reported in the literature (Fig. 1).^{61,62} The unsubstituted DBF compound **26** shows GR binding affinity, selectivity and agonist activity similar to the 2-methoxy-5-fluoro analogue **2** (Table 5). The effect of substitution at a position *para*- to the oxygen atom of the DBF ring was explored and the data is shown in Table 5. Groups such as F, Br and CH₃ do not alter the selectivity profile (**27–29**). However, cyano (**30**) and methylsulfone (**31**) substitution have a dramatic effect on GR/PR selectivity. While the cyano analogue **30** is 50-fold selective, the methylsulfone compound **31** shows greater than 300-fold selectivity over PR, and 100-fold selectivity over MR. The selectivity data can be rationalized using our docking studies.

Figure 5a and b show an overlay of the (*R*)-enantiomers of **31** and dexamethasone. In the A-ring region, no difference in the interactions with the GR–LBD is observed between (*R*)-**31** and (*R*)-**2** (Figs. 3a and 5a). However in the GR–LBD/(*R*)-**31** binding pose (Fig. 5b), the methylsulfone oxygen atoms of (*R*)-**31** lie in a space closer to the C-18 carbonyl of dexamethasone and potential hydrogen bonding to the side chain hydroxyl of Thr739 is

implicated. Some of the amino acid residue differences between GR and PR in the D-ring domain could explain the observed GR/PR selectivity. Two residues, Met639 and Gln642 are proximal to the dihydrofuran ring (of DBF moiety) at the RHS. The corresponding residues in PR are Phe794 and Leu797, respectively. As a result the PR binding pocket is reduced in size and may not accommodate both the dihydrofuran ring and the bulkier methylsulfone group. Thus, PR binding is eroded leading to enhanced GR/PR selectivity.

In the transrepression assay, F, Br and CH₃ analogues (**27–29**, Table 5) show activity similar to the unsubstituted DBF analogue **26**. The CN-DBF and methylsulfone-DBF analogues **30** and **31**, respectively, display 10-fold loss in transrepression potency as compared to **26**. In contrast to the indole analogues, DBF analogues show more separation in the TA and TR activity. Compounds **26**, **27** and **30** show a 3–30-fold difference in EC₅₀/IC₅₀. The most striking result is the dissociated profile of the methylsulfone-DBF **31** analogue in the MMTV assay (EC₅₀ 2 μM, % maximum efficacy 20). The MMTV and nuclear receptor selectivity data for **31** in combination with the results for the DBF compounds **26**, **27** and **30** suggesting a trend towards separation in the TA (aromatase data) and TR activity prompted us to choose methylsulfone-DBF as the RHS for further modifications, despite the lack of aromatase data for **31**. These results highlight the methylsulfone-DBF as an FRP mimicking the steroidal D-ring.

With the goal of generating optimal compounds for in vivo evaluation, we prepared compounds combining the FRPs at the LHS and RHS of the molecule that gave better nuclear receptor selectivity and dissociation. Based on the results discussed earlier, methylsulfone-DBF RHS and both the 5-CN and 6-CN indole LHS were employed to prepare **32** and **33**. Compounds **32** and **33** display high GR affinity and selectivity over PR, MR and both the cyano compounds are 2-fold more potent in the IL-6 transrepression assay compared to the methylsulfone-DBF unsubstituted indole **31** (Table 6). The 6-Cyano compound **33** was resolved on a chiral column and the data for the enantiomers (*S*)-**33** and (*R*)-**33** is shown in Table 6. Both compounds **32** and **33** transactivate poorly in the MMTV assay (EC₅₀ 2 μM, % maximum efficacy <10). A smaller 2–3-fold separation in the EC₅₀/IC₅₀ is seen in the aromatase assay and both analogues maintain potent agonist properties. The eutomer (*R*)-**33** of the 6-CN analogue with more than 100-fold PR, MR and AR selectivity, an IL-6 IC₅₀ of 28 nM (% maximum efficacy 88) and full dissociation in the MMTV assay and a weak dissociation in the aromatase assay was chosen for in vivo profiling.

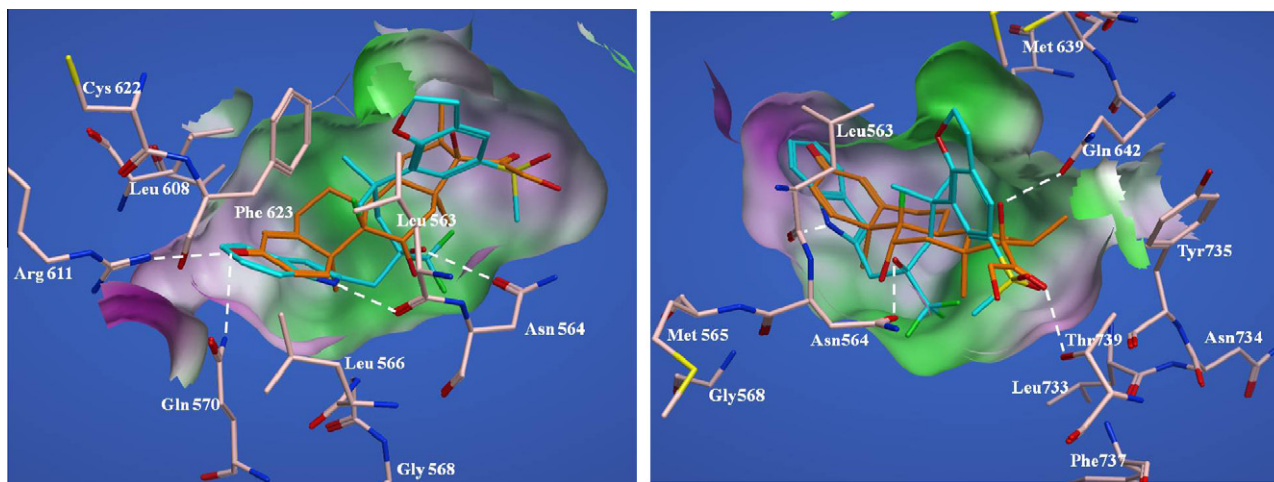
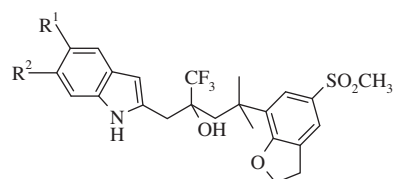
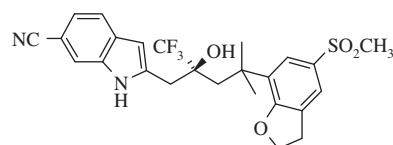
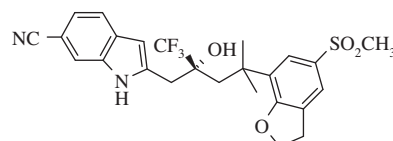


Figure 5. (a) (Left) and (b) (right): Docking poses for (*R*)-**31** (cyan) in the GR–LBD co-complex structure with dexamethasone⁴⁰ (orange). (a) Shows the region around the A-ring of dexamethasone, (b) Shows the region around the D-ring. Selected amino acids exhibiting key interactions with the ligand are shown. Potential H-bonds are indicated as dashed white lines.

Table 6Data on the Compounds **32**, **33**, (*S*)-**33** and (*R*)-**33** $R^1 = \text{CN}; R^2 = \text{H}$, **32** $R^1 = \text{H}; R^2 = \text{CN}$, **33***(S)*-**33***(R)*-**33**

Compd	IC ₅₀ (nM)				IC ₅₀ (nM) (% efficacy)		EC ₅₀ (nM), (% efficacy)	
	GR	PR	MR	AR	IL-6 inhibition	Aromatase induction	MMTV induction	
32	5	>2000	1450		49 (85)	80 (63)	>2000 (4)	
33	5	>2000	430		39 (89)	125 (98)	>2000 (10)	
<i>(S)</i> - 33	405	1400	405		—	—	—	
<i>(R)</i> - 33	2	745	230	NDB at 2000 nM	28 (88)	120 (74)	>2000 (10)	

(R)-**33** was evaluated for pharmacokinetic properties in mice and rats. Modest bioavailability in mice and rats (26% and 51%,

respectively) was observed with an acceptable half-life after oral dosing (Table 7).

Table 7Pharmacokinetic data of (*R*)-**33** in B10.RIII mice and Sprague-Dawley rats

	Mouse ^a	Rat ^b
iv CL (ml/min/kg)	4	51
V _{SS} (L/kg)	0.9	7.7
t _{1/2} (hr)	2.5	1.7
po C _{max} (ng/ml)	6187	955
po AUC _{inf} (hr ng/ml)	32729	4850
F (%)	26	51

^a Dosed at 1 mg/kg i.v. in a PEG400/water (70:30) vehicle and at 30 mg/kg po as a suspension in 30% Cremophor, mean of 3 mice.

^b Dosed at 2 mg/kg i.v. in a PEG400/water (70:30) vehicle and at 30 mg/kg po in a PEG400/H₂O/Tween (80/18/2) vehicle, mean of 3 rats.

Anti-inflammatory properties of a select panel of compounds, that includes the in vitro dissociated compounds **32**, **33** and (*R*)-**33**, were determined in an LPS-stimulated mouse model of TNF- α production. Test compounds were administered orally in Cremophor RH 1 h prior to LPS challenge and plasma TNF- α levels were measured 1 h after the challenge. Table 8 summarizes the data. The unsubstituted indole (*R*)-**2** did not show efficacy and the DBF analogues (*R*)-**29**, **32** and **33** displayed ED₅₀ less than 10 mg/kg. (*R*)-**33** completely inhibited TNF- α production at 3 mg/kg. With an ED₅₀ of less than 3 mg/kg (*R*)-**33** represents a dissociated GR agonist displaying an anti-inflammatory efficacy equal to prednisolone in the LPS model.

(*R*)-**33** was also tested in a mouse model of collagen induced arthritis (CIA), a chronic model of inflammatory polyarthritis which shares many features with human rheumatoid arthritis.⁶³

Table 8

In vitro activities of indoles

Compd	IC ₅₀ (nM)	IC ₅₀ (nM) (% efficacy)	EC ₅₀ (nM), (% efficacy)	Inhibition of TNF- α in mice (%)(n=8) 3 and 10 mg/kg	
	GR	IL-6 inhibition in HFF	Aromatase Induction in HFF	3 mg/kg	10 mg/kg
Pred.	15	7 (96)	19 (92)	—	84
(<i>R</i>)- 2	10	6 (87)	18 (98)	—	35
(<i>R</i>)- 29	12	7 (92)	14 (120)	—	61
32	5	49 (85)	80 (63)	NE [*]	77
33	5	39 (89)	125 (98)	66	66
(<i>R</i>)- 33	2	28 (88)	120 (74)	97	88

* No efficacy.

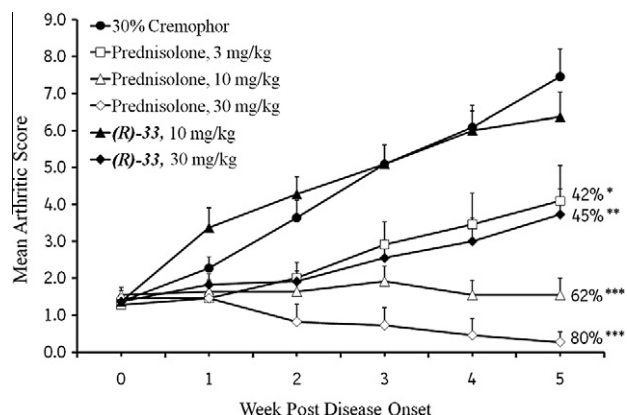


Figure 6. Collagen Induced Arthritis Model: (R)-33. Data are given as mean of 10 animals per group; Statistical analysis of AUCs was performed with the Mann-Whitney test: * $p < 0.05$, ** $p < 0.005$, *** $p < 0.0005$ compared to vehicle (30% Cremophor RH).

Table 9
Side effect profile of (R)-33 and prednisolone

	% Change relative to vehicle control		
	Prednisolone		(R)-33 30 mg/kg
	3 mg/kg	30 mg/kg	
Body weight	1.1	9 [#]	-8
% Body fat	36 [#]	70 [#]	6 ⁺⁺
Triglycerides	-11	55	11
Free fatty acid	8	25 [#]	8
Insulin	37	190 [#]	-29

[#] $p < 0.05$ t-Test versus vehicle control.

⁺⁺ $p < 0.05$ Versus prednisolone 3 mg/kg.

(R)-33 inhibited disease progression with the 30 mg/kg dose group exhibiting an efficacy (Mann-Whitney test: $p = 0.0028$) of 45% AUC inhibition as compared to the 80% for the 30 mg/kg prednisolone group. The efficacy obtained with the 30 mg/kg dose of (R)-33 was comparable to that of 3 mg/kg dose of prednisolone (Fig. 6).

To evaluate the in vivo side effect profile of (R)-33, body fat content was assessed by densitometry. Serum metabolic markers such as triglyceride, free fatty acid and insulin levels were analyzed and compared to results with prednisolone treatment. A significant dose dependent increase in body fat content was seen with prednisolone treatment at 3 and 30 mg/kg versus vehicle control (36%, 70%, respectively, relative to vehicle control; t -test: $p < 0.05$, Table 9). In contrast, no significant difference was observed with (R)-33 at 10 and 30 mg/kg (data shown for 30 mg/kg, 6% relative to vehicle control, Table 9). Importantly, at an equally efficacious anti-inflammatory dose (3 mg/kg for prednisolone and 30 mg/kg for (R)-33) a statistically significant smaller change of 6% in body fat content was observed for (R)-33 as compared to 36% for prednisolone. No statistically significant changes in serum metabolic markers were seen with (R)-33 at 10 or 30 mg/kg versus vehicle control (Table 9). These results could not be properly evaluated as doses higher than 30 mg/kg of (R)-33 are required to make a meaningful comparison with prednisolone which induces significant changes in serum markers only at doses higher than 3 mg/kg.

In summary, we have described SAR optimization of a non-steroidal GR agonist **2** with an indole as A-ring mimic. Our studies demonstrate that nuclear receptor selectivity, agonist activity and in vitro dissociation of the GR ligand **2** can be modulated by both the nature and position of the substitutions by the groups such as F, Me, CF₃, CN and methylsulfone. While selectivity over PR and MR, and in vitro dissociation is modulated by substitutions

on both the A- and D-ring regions of molecule **2** (LHS and RHS respectively), agonist activity is more influenced by A-ring substitutions. 5-CN and 6-CN substituted indole rings and a RHS methylsulfone-DBF moiety have been identified as function-regulating pharmacophores that provide the beneficial properties for the GR ligand **2**. Highlighting the potent anti-inflammatory properties of indole analogues is compound (R)-33 which is equipotent to prednisolone in a LPS-TNF model of inflammation. Furthermore in the mouse CIA model, (R)-33 slowed the progression of disease with an efficacy of 45% at 30 mg/kg. We have identified indole analogues of **2** that show a dissociated profile based on % maximal efficacy or EC₅₀ or both. To assess the significance of the observed in vitro dissociation, further in vivo evaluation of the compounds may be required. The results presented in the current studies open opportunities for further explorations on the non-steroidal GR agonist **2**, the results of which will be communicated in the future.

Acknowledgments

We thank Doris Riether, Derek Cogan and Steven Brunette for reviewing the manuscript. Thanks are also due to Eugene Hickey for his assistance in generating the docking poses.

References and notes

- Beck, I. M.; De, B. K.; Haegeman, G. *Trends Endocrinol. Metab.* **2011**.
- De, B. K.; Vanden, B. W.; Haegeman, G. *J. Neuroimmunol.* **2000**, *109*, 16.
- De Bosscher, K.; Haegeman, G.; Elewaut, D. *Curr. Opin. Pharmacol.* **2010**, *10*, 497.
- De Bosscher, K.; Beck, I. M.; Haegeman, G. *Brain, Behavior and Immunity* **2010**, *24*, 1035.
- De Bosscher, K. *J. Steroid Biochem. Mol. Biol.* **2010**, *120*, 96.
- De Bosscher, K.; Van Craenenbroeck, K.; Meijer, O. C.; Haegeman, G. *Eur. J. Pharmacol.* **2008**, *583*, 290.
- De, B. K.; Haegeman, G. *Mol. Endocrinol.* **2009**, *23*, 281.
- De, B. K.; Vanden Berghe, W.; Haegeman, G. *Mol. Endocrinol.* **2001**, *15*, 219.
- De, B. K.; Vanden Berghe, W.; Haegeman, G. *Oncogene* **2006**, *25*, 6868.
- De, B. K.; Vanden Berghe, W.; Vermeulen, K.; Plaisance, S.; Boone, E.; Haegeman, G. *Proc. Natl. Acad. Sci. U.S.A.* **2000**, *97*, 3919.
- Schäcke, H.; Döcke, W. D.; Asadullah, K. *Pharmacol. Ther.* **2002**, *96*, 23.
- Reichardt, H. M.; Tuckermann, J. P.; Göttlicher, M.; Vujic, M.; Weih, F.; Angel, P.; Herrlich, P.; Schutz, G. *EMBO J.* **2001**, *20*, 7168.
- Zhou, J.; Cidlowski, J. A. *Steroids* **2005**, *70*, 407.
- Clark, R. D.; Ray, N. C.; Williams, K.; Blaney, P.; Ward, S.; Crackett, P. H.; Hurley, C.; Dyke, H. J.; Clark, D. E.; Lockey, P.; Devos, R.; Wong, M.; Porres, S. S.; Bright, C. P.; Jenkins, R. E.; Belanoff, J. *Bioorg. Med. Chem. Lett.* **2008**, *18*, 1312.
- Jaroch, S.; Berger, M.; Huwe, C.; Krolkiewicz, K.; Rehwinkel, H.; Schächke, H.; Schmees, N.; Skuballa, W. *Bioorg. Med. Chem. Lett.* **2010**, *20*, 5835.
- Robinson, R. P.; Buckbinder, L.; Haugeto, A. I.; McNiff, P. A.; Millham, M. L.; Reese, M. R.; Schaefer, J. F.; Abramov, Y. A.; Bordner, J.; Chantigny, Y. A.; Kleinman, E. F.; Laird, E. R.; Morgan, B. P.; Murray, J. C.; Salter, E. D.; Wessel, M. D.; Yocum, S. A. *J. Med. Chem.* **2009**, *52*, 1731.
- Xiao, H. Y.; Wu, D. R.; Malley, M. F.; Gougoutas, J. Z.; Habte, S. F.; Cunningham, M. D.; Somerville, J. E.; Dodd, J. H.; Barrish, J. C.; Nadler, S. G.; Dhar, T. G. M. *J. Med. Chem.* **2010**, *53*, 1270.
- Zhang, X.; Li, X.; Allan, G. F.; Musto, A.; Lundeen, S. G.; Sui, Z. *Bioorg. Med. Chem. Lett.* **2006**, *16*, 3233.
- Diallo, H.; Angell, D. C.; Barnett, H. A.; Biggadike, K.; Coe, D. M.; Cooper, T. W. J.; Craven, A.; Gray, J. R.; House, D.; Jack, T. I.; Keeling, S. P.; MacDonald, S. J. F.; McLay, I. M.; Oliver, S.; Taylor, S. J.; Uings, I. J.; Wellaway, N. *Bioorg. Med. Chem. Lett.* **2011**, *21*, 1126.
- Hudson, A. R.; Higuchi, R. I.; Roach, S. L.; Adams, M. E.; Vassar, A.; Syka, P. M.; Mais, D. E.; Miner, J. N.; Marschke, K. B.; Zhi, L. *Bioorg. Med. Chem. Lett.* **2011**, *21*, 1697.
- Hudson, A. R.; Higuchi, R. I.; Roach, S. L.; Valdez, L. J.; Adams, M. E.; Vassar, A.; Rungta, D.; Syka, P. M.; Mais, D. E.; Marschke, K. B.; Zhi, L. *Bioorg. Med. Chem. Lett.* **2011**, *21*, 1654.
- Roach, S. L.; Higuchi, R. I.; Hudson, A. R.; Adams, M. E.; Syka, P. M.; Mais, D. E.; Miner, J. N.; Marschke, K. B.; Zhi, L. *Bioorg. Med. Chem. Lett.* **2011**, *21*, 168.
- Roach, S. L.; Higuchi, R. I.; Hudson, A. R.; Vassar, A.; Grant, V. H. S.; Lamer, R.; Hooper, C.; Rungta, D.; Syka, P. M.; Mais, D. E.; Marschke, K. B.; Zhi, L. *Bioorg. Med. Chem. Lett.* **2011**, *21*, 1658.
- Biggadike, K.; Boudjelal, M.; Clackers, M.; Coe, D. M.; Demaine, D. A.; Hardy, G. W.; Humphreys, D.; Inglis, G. G. A.; Johnston, M. J.; Jones, H. T.; House, D.; Loiseau, R.; Needham, D.; Skone, P. A.; Uings, I.; Veitch, G.; Weingarten, G. G.; McLay, I. M.; MacDonald, S. J. F. *J. Med. Chem.* **2007**, *50*, 6519.
- Mohler, M. L.; He, Y.; Wu, Z.; Hong, S. S.; Miller, D. D. *Expert Opin. Ther. Pat.* **2007**, *17*, 37.

26. Regan, J.; Razavi, H.; Thomson, D. In *Annual Reports in Medicinal Chemistry*; Doherty, A. M., Ed.; Academic Press: New York, 2008; pp 141–154.
27. Berlin, M. *Expert Opin. Ther. Pat.* **2010**, *20*, 855.
28. Schäcke, H.; Berger, M.; Hansson, T. G.; McKercher, D.; Rehwinkel, H. *Expert Opin. Ther. Pat.* **2008**, *18*, 339.
29. Schäcke, H.; Asadullah, K.; Berger, M.; Rehwinkel, H. In *Nuclear Receptors as Drug Targets*; Ottow, E., Weinmann, H., Eds.; Wiley-VCH Verlag GmbH & Co. KGaA: Weinheim, Germany, 2008; pp 305–323.
30. Madauss, K. P.; Bledsoe, R. K.; Mclay, I.; Stewart, E. L.; Uings, I. J.; Weingarten, G.; Williams, S. P. *Bioorg. Med. Chem. Lett.* **2008**, *18*, 6097.
31. Biggadike, K.; Bledsoe, R. K.; Coe, D. M.; Cooper, T. W. J.; House, D.; Iannone, M. A.; MacDonald, S. J. F.; Madauss, K. P.; Mclay, I. M.; Shipley, T. J.; Taylor, S. J.; Tran, T. B.; Uings, I. J.; Weller, V.; Williams, S. P. *Proc. Natl. Acad. Sci. U.S.A.* **2009**, *106*, 18114.
32. Betageri, R.; Zhang, Y.; Zindell, R. M.; Kuzmich, D.; Kirrane, T. M.; Bentzien, J.; Cardozo, M.; Capolino, A. J.; Fadra, T. N.; Nelson, R. M.; Paw, Z.; Shih, D. T.; Shih, C. K.; Zuvella-Jelaska, L.; Nabozny, G.; Thomson, D. S. *Bioorg. Med. Chem. Lett.* **2005**, *15*, 4761.
33. Bekkali, Y.; Cardozo, M. G.; Kirrane, T. M.; Kuzmich, D.; Proudfoot, J. R.; Takahashi, H.; Thomson, D.; Wang, J.; Zindell, R.; Harcken, C. H. J. J.; Razavi, H. WO 03082787, 2003.
34. Kuzmich, D.; Kirrane, T.; Proudfoot, J.; Bekkali, Y.; Zindell, R.; Beck, L.; Nelson, R.; Shih, C. K.; Kukulka, A. J.; Paw, Z.; Reilly, P.; Deleon, R.; Cardozo, M.; Nabozny, G.; Thomson, D. *Bioorg. Med. Chem. Lett.* **2007**, *17*, 5025.
35. Bekkali, Y.; Betageri, R.; Gilmore, T. A.; Cardozo, M. G.; Kirrane, T. M.; Kuzmich, D.; Proudfoot, J. R.; Takahashi, H.; Thomson, D.; Wang, J.; Zindell, R.; Harcken, C. H. J. J.; Riether, D. Patent WO 03082280A1, 2003.
36. In addition to our discovery of indole as A-ring mimetic, research at Boehringer Ingelheim identified quinol-4-ones and azaindoles as attractive A-ring replacements. These are exemplified by the compounds **3** and **4**, respectively. These discoveries were published in the recent articles. See Ref. 45,46.
37. Glide, version 5.0, Schrödinger, LLC, New York, NY, **2008**.
38. (R)-**2** and (R)-**31** were docked into the GR-LBD pocket using the GR-LBD/dexamethasone co-complex X-ray structure.⁴⁰ The docking studies were done using the Glide³⁷ and Figures 3a and 3b, 5a and 5b were prepared using MOE.³⁹
39. Molecular Operating Environment (MOE), 2010.10; Chemical Computing Group Inc., 1010 Sherbrooke St. West, Suite #910, Montreal, QC, Canada, H3A 2R7, **2010**.
40. Bledsoe, R. K.; Montana, V. G.; Stanley, T. B.; Delves, C. J.; Apolito, C. J.; McKee, D. D.; Conser, T. G.; Parks, D. J.; Stewart, E. L.; Willson, T. M.; Lambert, M. H.; Moore, J. T.; Pearce, K. H.; Xu, H. E. *Cell* **2002**, *110*, 93.
41. Barker, M.; Clackers, M.; Copley, R.; Demaine, D. A.; Humphreys, D.; Inglis, G. G. A.; Johnston, M. J.; Jones, H. T.; Haase, M. V.; House, D.; Loiseau, R.; Nisbet, L.; Pacquet, F.; Skone, P. A.; Shanahan, S. E.; Tape, D.; Vinader, V. M.; Washington, M.; Uings, I.; Upton, R.; Mclay, I. M.; MacDonald, S. J. F. *J. Med. Chem.* **2006**, *49*, 4216.
42. Barker, M.; Clackers, M.; Demaine, D. A.; Humphreys, D.; Johnston, M. J.; Jones, H. T.; Pacquet, F.; Pritchard, J. M.; Salter, M.; Shanahan, S. E.; Skone, P. A.; Vinader, V. M.; Uings, I.; Mclay, I. M.; Macdonald, S. J. *J. Med. Chem.* **2005**, *48*, 4507.
43. Tucker, H.; Crook, J. W.; Chesterson, G. J. *J. Med. Chem.* **1998**, *31*, 954.
44. Fensome, A.; Bender, R.; Chopra, R.; Cohen, J.; Collins, M. A.; Hudak, V.; Malakian, K.; Lockhead, S.; Olland, A.; Svenson, K.; Terefenko, E. A.; Unwalla, R. J.; Wilhelm, J. M.; Wolfrom, S.; Zhu, Y.; Zhang, Z.; Zhang, P.; Winneker, R. C.; Wrobel, J. *J. Med. Chem.* **2005**, *48*, 5092.
45. Riether, D.; Harcken, C.; Razavi, H.; Kuzmich, D.; Gilmore, T.; Bentzien, J.; Pack, E. J.; Souza, D.; Nelson, R. M.; Kukulka, A.; Fadra, T. N.; Zuvella-Jelaska, L.; Pelletier, J.; Dinallo, R.; Ranzienbeck, M.; Torcellini, C.; Nabozny, G. H.; Thomson, D. S. *J. Med. Chem.* **2010**, *53*, 6681.
46. Regan, J.; Lee, T. W.; Zindell, R. M.; Bekkali, Y.; Bentzien, J.; Gilmore, T.; Hammach, A.; Kirrane, T. M.; Kukulka, A. J.; Kuzmich, D.; Nelson, R. M.; Proudfoot, J. R.; Ralph, M.; Pelletier, J.; Souza, D.; Zuvella-Jelaska, L.; Nabozny, G.; Thomson, D. S. *J. Med. Chem.* **2006**, *49*, 7887.
47. Lee, T. W.; Proudfoot, J. R.; Thomson, D. S. *Bioorg. Med. Chem. Lett.* **2006**, *16*, 654.
48. GR, PR and MR binding assays measured competition between test compound and fluorescently labeled probes for binding to recombinant human receptors in cell lysates made from baculovirus-infected insect cells. The probes used for the assays were as follows. GR and MR assays: 5 nM tetramethylrhodamine-labeled dexamethasone; PR assay: 5 nM tetramethylrhodamine-labeled RU-486. The DMSO concentration in all binding reactions was 1% (v/v) and binding reactions were incubated for one hour at room temperature before measuring fluorescence polarization signal. The signal produced by maximal inhibition (background signal) was determined in wells containing 2 mM reference inhibitor for each receptor: dexamethasone for GR and MR, RU-486 for PR. Fluorescence polarization signals from duplicate 11-point concentration-response curves were fitted to a 4-parameter logistic equation to determine IC₅₀ values. AR binding assays measured competition between test compound at a single concentration and 10 nM concentration of ³H-testosterone for binding to recombinant human receptor in cell lysates made from baculovirus-infected cells. Dihydrotestosterone at 2 μM concentration was employed as the positive control. Results with compounds **2**, (R)-**2** and (R)-**33** showed 100% of control, demonstrating no measurable displacement of ³H-testosterone to the receptor.
49. Waage, A.; Slupphaug, G.; Shalaby, R. *Eur. J. Immunol.* **1990**, *20*, 2439.
50. The fibroblast-IL-6 assay measured the ability of test compounds to inhibit the elaboration of IL-6 by human foreskin fibroblasts (ATCC # CRL-2429) following stimulation by IL-1 (1 ng/mL) in vitro. After incubation at 37 °C for 18–24 h, IL-6 concentration in the tissue culture media was measured using standard electrochemiluminescence, DELFIA, or ELISA methods. In this assay, IL-6 inhibition is a measure of glucocorticoid receptor response to agonist, and dexamethasone was assigned 100% efficacy.
51. Berkovitz, G. D.; Bisat, T.; Carter, K. M. *J. Steroid Biochem.* **1989**, *33*, 341.
52. The fibroblast-aromatase assay measured the ability of test compounds to induce aromatase activity in human foreskin fibroblasts, as indicated by the production of β-estradiol from exogenously added testosterone (1 μM). After incubation at 37 °C for 18–24 h, estradiol concentration in the cell culture media was measured using a commercial ELISA (ALPCO # 020-DR-2693). Dexamethasone maximally induced aromatase activity and related estradiol production in this assay, and displayed a mean EC₅₀ value of 1.8 nM.
53. The HeLa MMTV transactivation assay measured the ability of test compounds to activate MMTV promoter in HeLa cells stably transfected with a MMTV-luciferase construct. Following addition of test compounds, plates were incubated for 6 h at 37 °C and 5% CO₂ and luminescent signal was detected in lysed cells using Steady-Glo[®] luciferase reagents (Promega #E2520). Dexamethasone (1 μM) was assigned 100% induction of luminescent signal in this assay.
54. Buetti, E.; Diggelmann, H. *Cell* **1981**, *23*, 335.
55. Buetti, E.; Kuhnel, B. *J. Mol. Biol.* **1986**, *190*, 379.
56. Ringold, G. M.; Yamamoto, K. R.; Tomkins, G. M.; Bishop, M.; Varmus, H. E. *Cell* **1975**, *6*, 299.
57. Ringold, G. M.; Dobson, D. E.; Grove, J. R.; Hall, C. V.; Lee, F.; Vannice, J. L. *Recent Prog. Horm. Res.* **1983**, *39*, 387.
58. Coghlan, M. J.; Elmore, S. W.; Kym, P. R.; Kort, M. E. In *Annual Reports in Medicinal Chemistry*; Doherty, A. M., Ed.; Academic Press, 2002; pp 167–176.
59. Thompson, C. F.; Quraishi, N.; Ali, A.; Tata, J. R.; Hammond, M. L.; Balkovec, J. M.; Einstein, M.; Ge, L.; Harris, G.; Kelly, T. M.; Mazur, P.; Pandit, S.; Santoro, J.; Sitlani, A.; Wang, C.; Williamson, J.; Miller, D. K.; Yamin, T. T.; Thompson, C. M.; O'Neill, E. A.; Zaller, D.; Forrest, M. J.; Carballo-Jane, E.; Luell, S. *Bioorg. Med. Chem. Lett.* **2005**, *15*, 2163.
60. Smith, C. J.; Ali, A.; Balkovec, J. M.; Graham, D. W.; Hammond, M. L.; Patel, G. F.; Rouen, G. P.; Smith, S. K.; Tata, J. R.; Einstein, M.; Ge, L.; Harris, G. S.; Kelly, T. M.; Mazur, P.; Thompson, C. M.; Wang, C. F.; Williamson, J. M.; Miller, D. K.; Pandit, S.; Santoro, J. C.; Sitlani, A.; Yamin, T. T.; O'Neill, E. A.; Zaller, D. M.; Carballo-Jane, E.; Forrest, M. J.; Luell, S. *Bioorg. Med. Chem. Lett.* **2005**, *15*, 2926.
61. Schäcke, H.; Zollner, T. M.; Docke, W. D.; Rehwinkel, H.; Jaroch, S.; Skuballa, W.; Neuhaus, R.; May, E.; Zogel, U.; Asadullah, K. *Brit. J. Pharmacol.* **2009**, *158*, 1088.
62. Schäcke, H.; Schottelius, A.; Docke, W. D.; Strehlke, P.; Jaroch, S.; Schmees, N.; Rehwinkel, H.; Hennekes, H.; Asadullah, K. *Proc. Natl. Acad. Sci. U.S.A.* **2004**, *101*, 227.
63. B10.RIII mice were immunized with porcine type II collagen and complete Freund's adjuvant then monitored for signs of arthritis. Animals were enrolled into the study at the first signs of disease and treated daily with compound, prednisolone or vehicle for a period of 5 weeks. The animals were monitored regularly and arthritis severity was assessed through clinical scoring of all four paws based on a score of 1–4. The clinical score per paw was summed to give a maximal severity score of 16 for each animal. (R)-**33** were evaluated in the model at once daily oral doses of 30 and 10 mg/kg for a period of 5 weeks versus prednisolone at 30, 10 and 3 mg/kg. At termination (day 35), the animal was anesthetized with 50 mg/kg (10 mg/ml) Ketamine/15 mg/kg (2 mg/ml) Zylazine. A whole body non-invasive density scan was performed to assess body fat content. (PIXImus densitometer, Lunar Corp.). Serum samples were collected for biomarker analysis. Triglyceride levels were determined with the Wako L-Type TG-H kit (Wako Diagnostics, Richmond, VA). Free fatty acids in serum were measured using the Wako NEFA-C Microtiter Procedure (Wako Diagnostics, Richmond, VA, Catalog #994-75409). For the serum insulin assay, the Ultra Sensitive Rat Insulin ELISA Kit (Crystal Chem Inc., Chicago, IL, Catalog #90060) and Mouse Insulin Standard 1.28 ng (Catalog #90090) was used.